Quantum vortex dynamics in a Josephson junction array frustrated by external charges

G Luciano†, U Eckern‡, J G Kissner‡ and A Tagliacozzo†

† Dipartimento di Scienze Fisiche, Universita' di Napoli e INFM, Mostra d'Oltremare, Padiment 19, I-80125 Napoli, Italy
‡ Institut für Physik, Universität Augsburg, D-86135 Augsburg, Germany

Abstract. We study the effect of a uniform background of external charges on the superconductor–insulator phase transition and on single-vortex properties, such as mass and damping, in a quantum (zero-temperature) Josephson junction array, in the case of long-range Coulomb interaction between Cooper pairs. We find, by an analytical method based on a small-α ($\alpha^2 = E_C/8E_J$) expansion, that the phase transition moves quickly to higher α with increasing offset charge, indicating that external charges significantly stabilize the superconducting phase. At the transition the vortex mass vanishes and the spin-wave damping decreases, as a consequence of the suppression of charge fluctuations, while upon decreasing α, we confirm the 'classical' result for the mass and the damping, independently of the external charges.

1. Introduction

In recent years much attention has been devoted to the study of Josephson junction arrays (JJA) [1], because, in ultrasmall junctions, charging effects lead to the observation of quantum properties at the macroscopic level. Furthermore, due to the fact that junction parameters can be controlled accurately and disorder is weak, Josephson junction arrays offer a unique opportunity to test models of quantum statistical mechanics.

In particular, such an array can undergo a superconductor–insulator transition at low temperature [2, 3, 4], when the Coulomb charging energy E_C becomes comparable to the Josephson coupling energy E_J ($\alpha = \sqrt{E_C/8E_J} \sim 1$). The transition separates two phases: in the superconducting phase, vortices, that are topological excitations of the phase, are bound in dipoles of opposite vorticity and Cooper pairs are delocalized, while in the insulating phase, Cooper pairs are localized and the phase becomes delocalized. The transition has been studied numerically and analytically in [5] using a description in terms of the topological excitations of the system, charges and vortices. In this formulation various collective properties in the superconducting phase can be analysed; in particular, the dynamics of a single vortex can be studied.

The presence of offset charges on the metallic islands can be a problem in the experiments. Presumably they are induced by trapped impurities in the substrate, and generally are hard to avoid. Furthermore an external gate voltage applied between the array and the substrate has a similar effect. Several authors [6, 7] have studied the phase diagram in the presence of external charges for a short-ranged Coulomb interaction; much less is known when the interaction is long range. Nevertheless, the latter case is relevant

for some of the arrays investigated experimentally [2, 8], as well as being very interesting theoretically.

Motivated by this problem, we study in this article the influence of a static background of external charges on the superconductor–insulator phase transition and on the quantum vortex dynamics in a Josephson junction array. We assume that the capacitance between islands, C_1, is much larger than the ground capacitance, C_0. Of course, a homogeneous background represents only a poor approximation of the real distribution of charges due to the impurities, but it is a first step, and we expect insights into the general problem.

To investigate the system, we use the method introduced in [9], which, in particular, preserves two essential features of the model: the discreteness of charge transfer (by Cooper pairs) between islands, and the invariance of the system, when all external charges are increased by a multiple of $2e$, leading to the expected periodicity of all physical quantities. This method is based on the approach described in [3, 5], where by a Villain transformation [10, 11] the partition function is expressed as a collection of vortex–antivortex pairs. In section 2 we use this approach to obtain an expression for the charge–charge correlation function, which plays the main role in studying the transition and in determining various aspects of the vortex dynamics. Section 3 is devoted to the evaluation of this quantity on the superconducting side, by an analytical method, similar to a low-temperature expansion. For large Josephson coupling, $E_J \gg E_C$, the charge–charge correlation function reduces to its classical limit form, independently of the offset charges, confirming the continuum limit results for mass and damping of the vortex. This means that, for a large value of the ratio E_J/E_C, the charges can flow in a continuous fashion across the junctions. The superconductor–insulator transition is discussed in section 4. It is strongly affected by the offset charges and moves quickly to smaller E_J/E_C when the magnitude of the external charges is increased. In particular, it seems to disappear for a large enough charge. The dynamics of an individual vortex added to the array is studied in section 5. We calculate its mass and study the possibility of ballistic motion when an external current is applied to the array. We show that, with increasing offset charge, the vortex mass increases and the ballistic regime is less likely to be observable.

2. Description of the model

We consider a system of superconducting grains, which form a two-dimensional square lattice with lattice constant $a = 1$, coupled by Josephson junctions. The relevant variables of the model are the phases of the superconducting order parameter, $\{\varphi_i\}$ (the index $i = (i_x, i_y)$ labels the islands) and their conjugate variables, which are the charges, $\{2en_i\}$: $[n_k, \phi_l] = -i\delta_{kl}$. Introducing static (generally noninteger) *external* charges, $\{2eq_i\}$, on each island, the quantum Hamiltonian of the array is given by

$$\mathcal{H} = \frac{1}{2}(2e)^2 \sum_{ij}(n_i - q_i)\mathcal{C}_{ij}^{-1}(n_j - q_j) - E_J \sum_{(i,j)} \cos(\varphi_i - \varphi_j). \tag{1}$$

The Josephson coupling energy, E_J, is related to the critical current of a single junction, $E_J = \hbar I_J/2e$, and $\mathcal{C}_{ij}^{-1}$ is the inverse of the capacitance matrix. We take only the ground capacitance, C_0, into account, and the capacitance between neighbouring islands, C_1 ($E_C = e^2/2C_1$). Thus the only nonvanishing elements are $\mathcal{C}_{ii} = C_0 + 4C_1$ and $\mathcal{C}_{ij} = -C_1$ (ij nearest neighbours). Note that, in the long-wavelength limit, the Fourier transform of $\mathcal{C}_{ij}$ is given by

$$\mathcal{C}(\boldsymbol{k}) = C_0 + C_1 k^2 \tag{2}$$

so, for distances which are large compared to the lattice spacing, the Coulomb interaction in real space ($r = |r_i - r_j|$, with $r_i = (i_x, i_y)$) is

$$C^{-1}(r) = \frac{1}{2\pi C_1} K_0(r/\lambda) \tag{3}$$

which identifies $\lambda = (C_1/C_0)^{1/2}$ as the screening length. We assume below that $C_1 \gg C_0$ which means a long-range Coulomb interaction between the Cooper pairs.

In the superconducting phase the partition function can be expressed as a collection of vortex–antivortex pairs of vorticity $v_{i\tau}$ (the vorticity at each space-time point can take the values 0 or ± 1) [3]. A cumulant expansion yields the partition function in the following form [5]:

$$\mathcal{Z} = \mathcal{Z}_n \sum_{\{v_{j\tau}\}} e^{-\tilde{S}_0 - \tilde{S}_1} \tag{4}$$

with

$$\tilde{S}_0 = \frac{\pi E_J}{\omega_p} \sum_{ij,\tau} v_{i\tau} G_{ij} v_{j\tau} \tag{5}$$

and

$$\tilde{S}_1 = \frac{1}{2} \sum_{ij,\tau} \sum_{kl,\tau'} \mathcal{Q}_{ij,\tau\tau'} \Theta_{ik} \Theta_{jl} \dot{v}_{k\tau} \dot{v}_{l\tau'} - i \sum_{ij,\tau} \langle n_{i\tau} \rangle \Theta_{ij} \dot{v}_{j\tau} \tag{6}$$

where $\omega_p = \sqrt{8 E_C E_J}$ is the Josephson plasma frequency (its inverse is chosen to define the time spacing, $\epsilon = \omega_p^{-1}$; $\hbar = 1$), and $G_{ij} = -\ln|r_i - r_j|$ is the logarithmic vortex–vortex interaction. Here, and in the following, a dot means a discrete, dimensionless time derivative. Furthermore, we defined the phase configuration around a vortex, $\Theta_{ij} = \arctan\big((y_i - y_j)/(x_i - x_j)\big)$, and the connected charge–charge correlation function, $\mathcal{Q}_{ij,\tau\tau'} = \langle (n_{i\tau} - q_i)(n_{j\tau'} - q_j) \rangle_c$. Averages $\langle\,.\,\rangle$ are performed with respect to the charge action:

$$S_n = \frac{1}{2} \sum_{ij,\tau\tau'} (n_{i\tau} - q_i) \mathcal{M}_{ij,\tau\tau'} (n_{j\tau'} - q_j). \tag{7}$$

$\mathcal{Z}_n = \text{Tr}[\exp(-S_n)]$, and the matrix $\mathcal{M}$ is defined by [5]

$$\mathcal{M}_{ij,\tau\tau'} = \frac{4 E_C}{\pi \omega_p} V_{ij} \delta_{\tau,\tau'} + \frac{\omega_p}{2\pi E_J} G_{ij} \left(2\delta_{\tau,\tau'} - \delta_{\tau,\tau'+\epsilon} - \delta_{\tau,\tau'-\epsilon} \right) \tag{8}$$

where $V_{ij} = 2\pi C_1 \mathcal{C}_{ij}^{-1}$.

In order to evaluate $\mathcal{Q}_{ij,\tau\tau'}$ and $\langle n_{i\tau} \rangle$ explicitly, we perform a Poisson resummation. The averages are expressed in terms of discrete auxiliary fields, $\phi_{i\tau}$, that run over all integers, $\phi_{i\tau} = 0, \pm 1, \pm 2, \ldots$. The resulting expressions for $\langle n_{i\tau} \rangle$ and $\mathcal{Q}_{ij,\tau\tau'}$ are the following:

$$\langle n_{i\tau} \rangle = q_i + 2\pi i \sum_{j\tau'} \mathcal{M}_{ij,\tau\tau'}^{-1} \langle \phi_{j\tau'} \rangle \tag{9}$$

and

$$\mathcal{Q}_{ij,\tau\tau'} = \mathcal{M}_{ij,\tau\tau'}^{-1} - (2\pi)^2 \sum_{kl,\tau_1\tau_2} \mathcal{M}_{ik,\tau\tau_1}^{-1} \langle \phi_{k\tau_1} \phi_{l\tau_2} \rangle_c \mathcal{M}_{lj,\tau_2\tau'}^{-1} \tag{10}$$

where the new average $\langle\,.\,\rangle$ is performed with the action

$$S_\phi = 2\pi^2 \sum_{i,\tau\tau'} \phi_{i\tau} \mathcal{M}_{ij,\tau\tau'}^{-1} \phi_{j\tau'} - 2\pi i \sum_{i\tau} q_i \phi_{i\tau}. \tag{11}$$

The advantage of introducing the ϕ-fields is that, in the limit $\lambda \gg 1$, they interact through the short-ranged kernel

$$\mathcal{M}^{-1}_{ij,\tau\tau'} = \frac{1}{16\alpha} \left(-\nabla^2\right) e^{-\omega_p|\tau-\tau'|} \tag{12}$$

where ∇^2 denotes the Laplacian on the lattice. This simplifies the problem of calculating the correlation function, because, as described in the next section, we will apply an expansion method that would be inefficient for a long-range interaction. In Fourier space, $(i, \tau) \rightarrow (k, \omega)$, the kernel is given by $(\lambda \rightarrow \infty)$

$$\mathcal{M}^{-1}_{k,\omega} = \frac{\omega_p}{8\alpha} \frac{k^2}{\omega^2 + \omega_p^2}. \tag{13}$$

The action S_ϕ is invariant when the external charges are increased by a multiple of $2e$, leading to the expected periodicity of all of the physical quantities. This invariance is a direct consequence of the discreteness of the auxiliary fields ϕ (note that in the Gaussian approximation and in the self-consistent harmonic approximation [5] the periodicity is lost, because, for calculating the correlation functions, the fields are considered as continuous variables).

From now on we examine a homogeneous external charge, $q_i = q$. Clearly, $\nabla^2 \langle \phi_{i\tau} \rangle = 0$ independently of q, and hence, considering (9), $\langle n_{i\tau} \rangle = q$. Several features of the superconductor–insulator transition (see section 4), and various aspects of the quantum vortex dynamics, such as mass and damping (see section 5), are determined by the charge–charge correlation function. Thus, in the next section, we focus our attention on this quantity.

3. Charge–charge correlation functions

In the representation given by equation (10), the charge–charge correlation function $\mathcal{Q}_{ij,\tau\tau'}$ is expressed as a function of the fields $\phi_{i\tau}$; the first term on the right-hand side describes the classical contribution for the correlation function, whereas the second term takes into account the discreteness of the charge variables. It begins to be important when the overall phase coherence between the islands becomes small, i.e. with increasing α. In order to evaluate $\mathcal{Q}_{ij,\tau\tau'}$, we explicitly need the connected correlation function, $\mathcal{K}_{mn,\nu} = \langle \phi_{i\tau} \phi_{j\tau'} \rangle - \langle \phi_{i\tau} \rangle \langle \phi_{j\tau'} \rangle$, where $j = i + m\hat{x} + n\hat{y}$, $\tau' = \tau + \nu\epsilon$ (m, n, ν are integers; clearly, this quantity is independent of (i, τ)). Making the q-dependence explicit, we may write, for example,

$$\langle \phi_{i\tau} \phi_{j\tau'} \rangle = \left\langle \phi_{i\tau} \phi_{i+m\hat{x}+n\hat{y},\tau+\nu\epsilon} \cos\left(2\pi q \sum_{k\tau'} \phi_{k\tau'}\right) \right\rangle_0 \bigg/ \left\langle \cos\left(2\pi q \sum_{k\tau'} \phi_{k\tau'}\right) \right\rangle_0 \tag{14}$$

where the index 0 indicates that the averages are performed for $q = 0$.

3.1. The small-α expansion

$\mathcal{K}_{mn,\nu}$ can be calculated exactly for $\alpha = 0$, yielding $\mathcal{K}_{mn,\nu}(\alpha = 0) = 0$, as follows easily with the help of equation (11); this implies that $\mathcal{Q} = \mathcal{M}^{-1}$ in this limit. Thus, for dominant Josephson coupling, $E_J \gg E_C$, the charge–charge correlation function reduces to the classical contribution, independently of q, i.e. the discreteness of the charges does not affect $\mathcal{Q}_{ij,\tau\tau'}$. Of course, as a direct consequence of this result, all single-vortex properties tend to those obtained in the classical limit, $\alpha \rightarrow 0$. This disagrees with the result given in [5] on the basis of a Monte Carlo simulation and a self-consistent harmonic approximation

(SCHA), namely that $\mathcal{Q}_{ij,\tau\tau'}$ does not vanish for $\alpha \to 0$. We believe that this conclusion is physically unreasonable.

For finite but small α, $\mathcal{K}_{mn,\nu}$ is computed via a small-α expansion, similar to the low-temperature expansion [12]. Only a few sites are 'excited'; that is, we can compute the average by including only those configurations that have a small number of excitations. To be more precise, the ground state for the system is $\phi_{i\tau} = 0$ $\forall(i, \tau)$. Due to the form of the kernel in (11), there is an arbitrariness, $\phi_{i\tau} \to \phi_{i\tau} + m$ with m an integer, but this ambiguity is not important in the calculation of the configuration. The lowest excitation is obtained by considering only one site with the value $\phi_{i\tau} = \pm 1$ (the model is symmetric with respect to the sign of the fields $\phi_{i\tau}$). The degeneracy of a single excitation is N, where N is the total number of sites, and the cost of this unit step is $e^{-\pi^2/2\alpha}$. Additional configurations can be obtained by increasing the number of excitations and by changing their position in the space-time lattice. Configurations can be visualized as surfaces joining plaquettes at height $\phi_{i\tau}$ above the ground. Of course, for small α, configurations with equal $\phi_{i\tau}$ are favoured, and the surface tends to be smooth.

$\mathcal{K}_{mn,\nu}$ depends on the parameter α, the charge q, and the space-time distance between the sites. The first contributions, as obtained within the low-α expansion, are given below ($s = e^{-\pi^2/4\alpha}$):

$$
\begin{aligned}
\mathcal{K}_{00,0} = {} & 2\cos(2\pi q)s^2 + 8\cos(4\pi q)s^3 \\
& + [-8 - 12\cos(4\pi q) + 36\cos(6\pi q) + 8\cos(8\pi q)]s^4 + \mathrm{O}(s^5) \\
& + 2s^4 \sum_{\nu \neq 0} T_\nu^+ + \mathrm{O}(s^{4(1-1/4e)})
\end{aligned}
\tag{15}
$$

$$
\mathcal{K}_{10,0} = 2\cos(4\pi q)s^3 + [2 - 2\cos(4\pi q) + 12\cos(6\pi q) + 4\cos(8\pi q)]s^4 + \mathrm{O}(s^5) \tag{16}
$$

$$
\mathcal{K}_{11,0} = [4\cos(6\pi q) + 2\cos(8\pi q)]s^4 + \mathrm{O}(s^5) \tag{17}
$$

$$
\mathcal{K}_{20,0} = 2\cos(6\pi q)s^4 + \mathrm{O}(s^5) \tag{18}
$$

$$
\mathcal{K}_{00,\nu} = 2s^4 T_\nu^- \tag{19}
$$

where $T_\nu^\pm = [s^{4/e^{|\nu|}} - 1]\cos(4\pi q) \pm [s^{-4/e^{|\nu|}} - 1]$, and $e = 2.71 \ldots$. The terms with integer exponents of s refer to the excitations in the space directions, whereas those with noninteger exponents originate from excitations in the time direction.

3.2. Large α: the continuum approximation

For $\alpha \to \infty$ and in the absence of external charges, the correlation function $\mathcal{K}$ can be computed by treating the ϕ-fields as continuous variables. For example, $\langle\phi_{i\tau}\phi_{j\tau'}\rangle$ becomes

$$
\sum_\phi \phi_{i\tau}\phi_{j\tau'}e^{-S_\phi} \bigg/ \sum_\phi e^{-S_\phi} = \alpha \sum_\psi (\sqrt{\alpha})^{-N} \psi_{i\tau}\psi_{j\tau'}e^{-S_\psi} \bigg/ \sum_\psi (\sqrt{\alpha})^{-N} e^{-S_\psi} \tag{20}
$$

with

$$
S_\psi = 2\pi^2\alpha \sum_{sl,tt'} \psi_{st}\mathcal{M}_{sl,tt'}^{-1}\psi_{lt'} \tag{21}
$$

where $\psi = \phi/\sqrt{\alpha}$. If we now replace the sum over ψ by an integration, we obtain $\langle\phi_{j\tau'}\rangle = 0$, and

$$
\mathcal{K}_{ij,\tau\tau'} = \langle\phi_{i\tau}\phi_{j\tau'}\rangle = \mathcal{M}_{ij,\tau\tau'}/(2\pi)^2. \tag{22}
$$

Substituting this result in equation (10), we eventually obtain $\mathcal{Q}(\alpha \to \infty) = 0$. The extension of this approximation to the case of finite external charges is an open problem.

4. Phase transitions

The analysis of section 3 shows that the correlation function $\mathcal{K}$, and, consequently, $\mathcal{Q}$, behaves differently in the two limits, $\alpha \to 0$ and $\alpha \to \infty$. For small α, $\mathcal{K}$ approaches a constant as $r \to \infty$, while for large α, this correlation function diverges, $\mathcal{K}(r) = \mathcal{M}(r)/(2\pi)^2 \sim \ln(r)$. This indicates that in between, at a critical value α_c, the model shows a transition from a superconducting to an insulating phase, as argued before in the absence of external charges [3], similar to the roughening transition. This is clear when we replace the exponential time dependence in (12) by a δ-function. Considering for a moment $q = 0$, the action S_ϕ reduces to the discrete Gaussian model

$$S_\phi^{DG} = \frac{\pi^2}{8\alpha} \sum_\tau \sum_{(i,j)} (\phi_{i\tau} - \phi_{j\tau})^2 \tag{23}$$

where (i, j) means nearest-neighbour sites. This model has been studied in connection with the roughening transition of solid–solid interfaces [13, 14]. Any site of the array is characterized by a value of the ϕ-fields, the 'height', that is, in a lattice-gas model, a measure of the number of atoms in the column. The interaction energy is an increasing function of the difference in heights between two nearest-neighbour sites. For small α, configurations with equal $\phi_{i\tau}$ are favoured, and the surface is smooth. As α increases and approaches α_c, the heights at different sites become more fuzzy and the surface changes (it is said to become more 'rough') in such a way that two distant points have uncorrelated heights. The phase transition can be characterized by the behaviour of the correlation function $G(r) = \langle (\phi_{i,\tau} - \phi_{j,\tau})^2 \rangle$, relating the mean square height difference between two columns separated by the distance $r = |r_i - r_j|$. It coincides, except for a constant, with the correlation function $\mathcal{K}(r)$. Below the roughening transition, $\alpha < \alpha_c$, $G(r)$ has a finite asymptotic value as $r \to \infty$, indicating a finite interface width, while at and above the transition this correlation function diverges $\sim A(\alpha) \ln r$, with $A(\alpha)$ an increasing function of α.

When $q \neq 0$, the action S_ϕ does not reduce to a Gaussian model. However, the behaviour of the correlation function $\mathcal{K}(r)$ for small and large α is still obtained, suggesting that the offset charges should not change the type of the phase transition of the model. However, the roughening analogy certainly requires further investigations.

To study the phase transition, it is useful to transform to Fourier space $(i, \tau) \to (k, \omega)$. For large enough α, i.e. in the insulating regime, the correlation function, using equations (22) and (13), is given by

$$\alpha \gg \alpha_c: \qquad \omega_p \mathcal{K}_{k,\omega} = \frac{2\alpha}{\pi^2} \frac{\omega^2 + \omega_p^2}{k^2} \tag{24}$$

which gives the expected logarithmic divergence as $r \to \infty$. Furthermore, the prefactor increases linearly in α. For $\alpha < \alpha_c$, i.e. in the superconducting regime, the correlation function is obtained via the low-α expansion. If we restrict ourselves to the terms (15)–(19), the correlation function becomes

$$\omega_p \mathcal{K}_{k,\omega} = \mathcal{K}_{00,0} + 2(\cos k_x + \cos k_y)\mathcal{K}_{10,0} + 4\cos k_x \cos k_y\,\mathcal{K}_{11,0}$$
$$+ 2(\cos 2k_x + \cos 2k_y)\mathcal{K}_{20,0} + \sum_{\nu \neq 0} \cos(\nu\omega)\mathcal{K}_{00,\nu}. \tag{25}$$
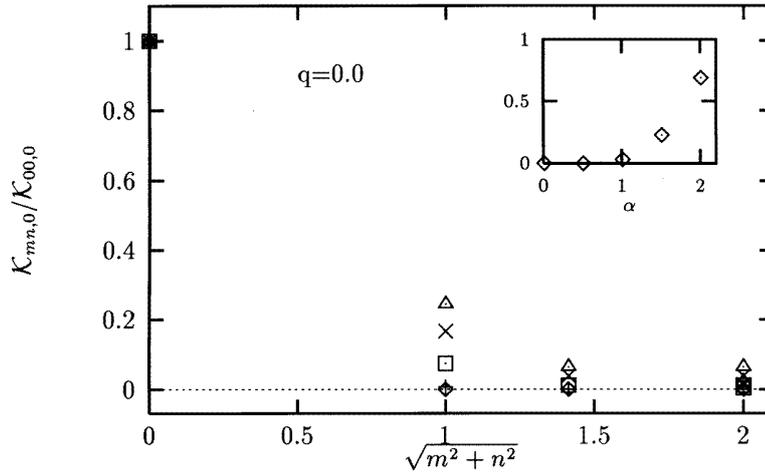
Figure 1. Normalized correlation functions $\mathcal{K}_{mn,\nu}$—compare equations (15)–(18)—for $q = 0.0$ versus space distance. The different symbols refer to different values of α ($\Diamond$: $\alpha = 0.0$; $+$: $\alpha = 0.5$; $\Box$: $\alpha = 1.0$; $\times$: $\alpha = 1.5$; $\triangle$: $\alpha = 2.0$). The inset shows the normalization, $\mathcal{K}_{00,0}$, for the same α-values.
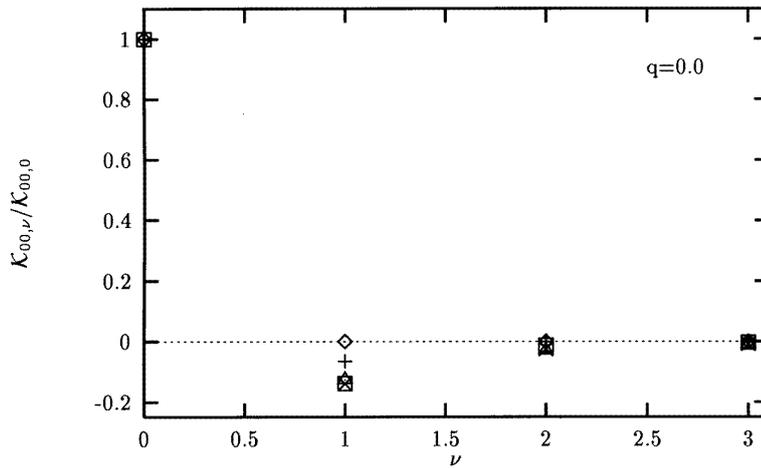

Figure 2. Normalized correlation functions $\mathcal{K}_{mn,\nu}$—compare equations (15) and (19)—for $q = 0.0$ versus time distance, for the same α-values as in figure 1.

Thus, for $k \to 0$, $\omega = 0$, it reduces to a constant, $\mathcal{K}_{k \to 0, \omega = 0} = \xi^2 \, 2\alpha/\pi^2 \omega_p + \mathrm{O}(k^2)$, which defines the correlation length, ξ. Explicitly,

$$
\xi^2 = \frac{\pi^2}{2\alpha} \left[2\cos(2\pi q)s^2 + 16\cos(4\pi q)s^3 \right.
$$

$$
\left. + [-20\cos(4\pi q) + 108\cos(6\pi q) + 32\cos(8\pi q)]s^4 \right.
$$

$$+ 4s^4 \sum_{\nu \neq 0} (s^{4/e^{|\nu|}} - 1) \cos(4\pi q) \tag{26}$$

In the last expression, we have taken into account for $\mathcal{K}_{mn,\nu}$ only the terms (15)–(19), and higher-order terms in the distance between the sites are disregarded. For not too large an external charge, $\mathcal{K}_{mn,\nu}$ is strongly peaked at $m = n = \nu = 0$, and falls off rapidly with increasing space or time distance (see figures 1 and 2). However, when q becomes too large, this is no longer true, and our approximation for evaluating ξ is not reliable. Furthermore, the terms with noninteger exponent, which originate from the excitations in the time direction, do not play a significant role in the calculation of ξ, and we neglect them in the following. Eventually,

$$\xi^2 = \frac{\pi^2}{2\alpha} \Big\{ 2\cos(2\pi q)s^2 + 16\cos(4\pi q)s^3$$
$$+ [-20\cos(4\pi q) + 108\cos(6\pi q) + 32\cos(8\pi q)]s^4 \Big\}. \tag{27}$$

The correlation length vanishes exponentially for $\alpha \to 0$, whereas it is expected to diverge at the transition. The series expansion gives ξ in the superconducting phase and not too near the critical value α_c, but strictly speaking does not allow the determination of its singularity. However, the knowledge of (27) is enough to extract information on the critical point by using, for example, the Padé approximant method [15]. The Padé approximations, $P_1^0(s)$, $P_2^0(s)$, and $P_1^1(s)$, for (27) are:

$$\xi_b^2 = \frac{\pi^2}{2\alpha} 2c_2 s^2 \qquad 1 - \frac{8c_4}{c_2}s \tag{28}$$

$$\xi_c^2 = \frac{\pi^2}{2\alpha} 2c_2 s^2 \Big/ \left\{ 1 - \frac{8c_4}{c_2}s + \left[\left(\frac{8c_4}{c_2} \right)^2 + \frac{10c_4 - 54c_6 - 16c_8}{c_2} \right] s^2 \right\} \tag{29}$$

$$\xi_d^2 = \frac{\pi^2}{2\alpha} \quad 2c_2 s^2 + \quad 16c_4 + \frac{(5c_4 - 27c_6 - 8c_8)c_2}{2c_4} \quad s^3 \qquad 1 + \frac{5c_4 - 27c_6 - 8c_8}{4c_4}s \tag{30}$$

where $c_n = \cos(n\pi q)$.

In figure 3 we show the results for ξ^2 as obtained from the series expansion (27) (curve a), and from ξ_b^2, ξ_c^2, and ξ_d^2 (the plots b, c, and d respectively) for $q = 0$. The behaviour of ξ^2 is qualitatively similar for the different Padé approximations even though the series (27) is rather short; in particular, the divergence is close to 1.2. This value is in reasonable agreement with the result $\alpha_c \simeq 1.05$ obtained with the SCHA approximation [5], but differs somewhat from other approaches, such as the duality argument [3] ($\simeq 0.79$), variational method [4] ($\simeq 0.5$), and Monte Carlo simulation [5] ($\simeq 0.46$). Note that the experimental data [2, 8] give $\simeq 0.5$ as the critical value.

To study the effect of the external charges on the phase transition, we work in the following with the diagonal Padé approximation, $P_1^1(s)$. In figure 4 we show the correlation length as a function of α for some values of q, in the range where our results are reliable. With increasing q, the divergence of ξ^2 moves quickly to higher α from the value $\alpha_c(q = 0) = 1.2$. This means that a finite external charge significantly stabilizes the superconducting phase. From these results, it is straightforward to determine the phase diagram in the variables q and $1/\alpha$, shown in figure 5. From the form of the phase diagram, we speculate that the transition almost disappears when the magnitude of the offset charge is strong enough.
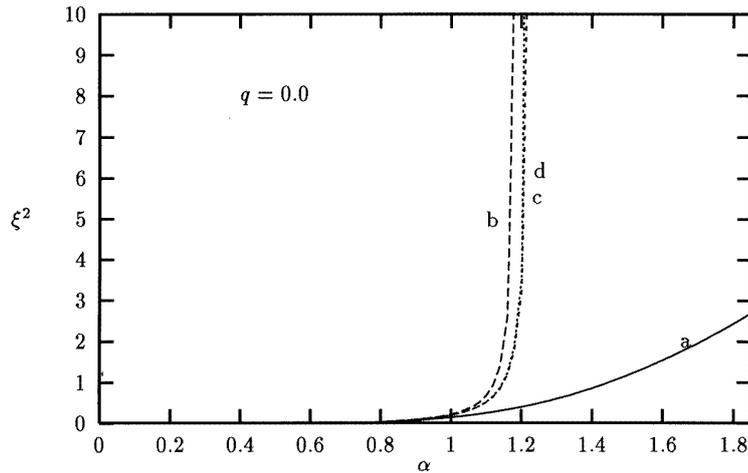
Figure 3. The squared correlation length versus α in the absence of external charges, based on equation (27), curve a, and for the three Padé approximations of this expression, $P_1^0(s)$, $P_2^0(s)$, and $P_1^1(s)$ (curves b–d, respectively).
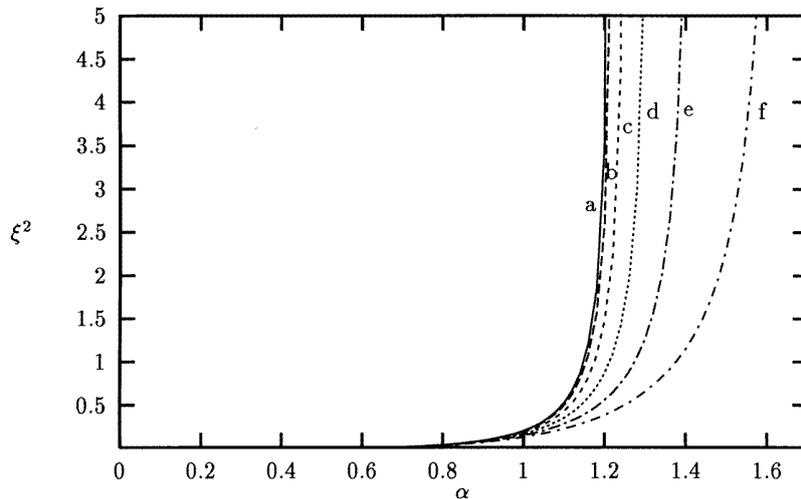

Figure 4. The squared correlation length versus α, on the basis of $P_1^1(s)$, for different values of the external charge. From a to f, q increases from 0.00 to 0.05 in steps of 0.01.

5. Quantum single-vortex dynamics

The aim of this section is to study the quantum properties of an individual vortex moving in the array. In the superconducting phase a small number of vortices can be induced by a small external magnetic field, and, when a current is applied, vortices experience a force and move. (For simplicity, we do not consider here the periodic potential due to the lattice.) An external uniform current $I(\tau)$ can be accounted for by adding to the action in the partition
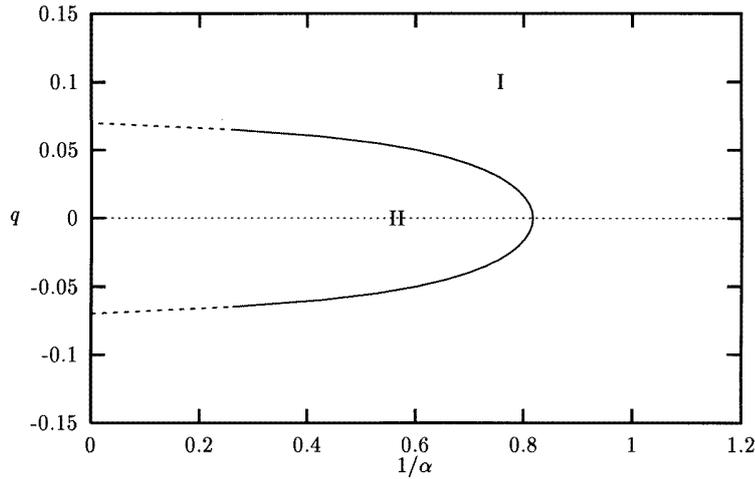
Figure 5. The phase diagram as a function of $1/\alpha$ and q. I: superconducting phase; II: insulating phase. The range of α-values where our approach is less reliable is shown with dashed lines.

function (4) the term [1]

$$\tilde{S}_2 = -\frac{2\pi\mathrm{i}}{\omega_p} \sum_{i\tau} \frac{\boldsymbol{I}(\tau)}{2e} \cdot (\hat{\boldsymbol{z}} \times \boldsymbol{r}_i) v_{i\tau} \tag{31}$$

If the magnetic frustration is small, we may suppose that the vortex motion is not influenced by their mutual interaction, and hence we focus our attention on an individual vortex with trajectory $\boldsymbol{r}(\tau)$ and configuration $v_{i\tau} = \delta(\boldsymbol{r}_i - \boldsymbol{r}(\tau))$. Its effective action (see equations (5), (6), and (31)) becomes $\mathcal{S}_{eff} = \mathcal{S}_v + \mathcal{S}_q + \mathcal{S}_I$, with

$$\mathcal{S}_v = \frac{1}{2} \sum_{\tau\tau'} \sum_{\alpha\beta} \dot{r}_\alpha(\tau) M_{\alpha\beta}[\boldsymbol{r}(\tau) - \boldsymbol{r}(\tau'), \tau - \tau'] \dot{r}_\beta(\tau') \tag{32}$$

$$\mathcal{S}_q = \mathrm{i}q \sum_{i\tau} \sum_{\alpha} \nabla_\alpha \Theta(\boldsymbol{r}(\tau) - \boldsymbol{r}_i) \dot{r}_\alpha(\tau) \tag{33}$$

$$\mathcal{S}_I = -\frac{2\pi\mathrm{i}}{\omega_p} \sum_{i\tau} \boldsymbol{f}(\tau) \cdot \left(\hat{\boldsymbol{z}} \times \boldsymbol{r}(\tau)\right) \tag{34}$$

where $\boldsymbol{f}(\tau) = \boldsymbol{I}(\tau)/2e$, and the vortex mass tensor is given by

$$M_{\alpha\beta}[\boldsymbol{r}(\tau) - \boldsymbol{r}(\tau'), \tau - \tau'] = \sum_{ij} \nabla_\alpha \Theta(\boldsymbol{r}(\tau) - \boldsymbol{r}_i) \mathcal{Q}_{ij,\tau\tau'} \nabla_\beta \Theta(\boldsymbol{r}_j - \boldsymbol{r}(\tau')). \tag{35}$$

5.1. The vortex mass

In the limit of a constant and small velocity, the action S_v reduces to that of a particle with mass

$$M_v = \omega_p^{-1} \sum_{\tau} M_{xx}(0, \tau) = \frac{1}{2} \int \frac{\mathrm{d}^2k}{k^2} \mathcal{Q}(\boldsymbol{k}, \omega = 0). \tag{36}$$

To clarify the concept of the vortex mass: when a vortex moves in the array, voltages across the junctions appear and, since the junctions have a capacitance C_1, electrostatic

energy is stored. This electrostatic energy can be interpreted [16, 17] as the kinetic energy of the vortex, which therefore has a mass M_v. Thus, M_v is proportional to the junction capacitance. Of course, the concept of a vortex mass only makes sense as long as the system is in the superconducting phase. It is expected that close to the superconductor–insulator transition the vortex mass will decrease rapidly as a consequence of the suppression of charge fluctuations, causing the vortex to become delocalized.

To evaluate the vortex mass, the Fourier transform of the charge–charge correlation function has to be computed. As obtained in section 3, $\mathcal{Q}_{k,\omega} = 0$ at the phase transition and hence, from equation (36), $M_v = 0$. The vanishing of the mass at the phase transition indicates that M_v in a sense describes the stability of the vortex configuration: it goes to zero when the vortex 'evaporates'.

In the limit $\alpha \to 0$, $\mathcal{Q}_{k,\omega} = \mathcal{M}_{k,\omega}^{-1}$. Substituting this result into equation (36), the vortex mass becomes

$$M_v = \frac{1}{2} \int \frac{\mathrm{d}^2 k}{k^2} \frac{k^2}{8\alpha\omega_p} = \frac{\pi^2}{4E_C} = M_{ES}. \tag{37}$$

This result is independent of the offset charge q; thereby we confirm the classical result [17], for all q.

Hence the vortex mass tends to a constant (M_{ES}) for large Josephson coupling E_J, and vanishes as α approaches the critical value α_c. In order to evaluate M_v in the intermediate area, we will assume that the connected correlation function $\mathcal{K}_{k,\omega}$ is of the form given by the SCHA approximation [5]:

$$\mathcal{K}_{k,\omega}^{SCHA} = \frac{2\alpha\omega_p}{\pi^2} \frac{(\omega^2 + \omega_p^2)\xi^2}{\omega^2 + \omega_p^2(1 + \xi^2 k^2)}. \tag{38}$$

Using equation (10), this implies (compare equation (13))

$$\mathcal{Q}(\boldsymbol{k}, \omega) = \frac{\omega_p}{8\alpha} \frac{k^2}{\omega^2 + \omega_k^2} \tag{39}$$

where $\omega_k^2 = \omega_p^2(1 + \xi^2 k^2)$. Thus ξ characterizes the stiffening of the spin-wave spectrum. Note, however, that as a direct consequence of the *ansatz* (39), we have for $\omega = 0$ and small k,

$$\mathcal{K}_{k,\omega=0}^{SCHA} \simeq \frac{2\alpha}{\omega_p \pi^2} \xi^2 (1 - \xi^2 k^2) \tag{40}$$

which we cannot confirm from our approximative result given in equation (25). Using equation (39), we compute the mass according to [5]

$$M_v/M_{ES} = (4\pi\xi^2)^{-1} \ln(1 + 4\pi\xi^2). \tag{41}$$

This expression is obtained using a sharp—symmetric—cut-off. Note that at the transition $\mathcal{K}_{k,\omega}^{SCHA}$ coincides with equation (24), while for small α, ξ is exponentially small and $\mathcal{K}_{k,\omega}^{SCHA}$ approaches a constant, as discussed above.

The vortex mass versus α for some values of the offset charges is shown in figure 6, using the Padé approximation $P_1^1(s)$, from equation (30).

5.2. Spin-wave damping and the ballistic regime

The notion of a massive vortex leads us to the question of whether or not a vortex can move ballistically in the array. This question has recently attracted considerable attention, experimentally [18] as well as theoretically [19, 20]. In high-quality JJA, where ohmic
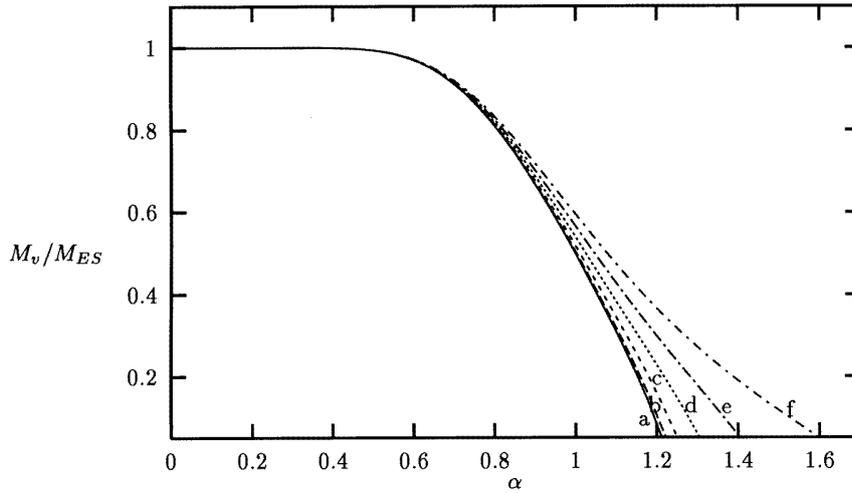
Figure 6. The vortex mass (normalized to M_{ES}) versus α, as calculated from equation (41), for the same q-values as in figure 4.

dissipation is negligibly small, and at a temperature low enough to freeze out quasiparticle excitations, the main mechanism of friction is the coupling of the vortex to the plasma oscillations: a moving vortex can lose its kinetic energy by emitting spin waves. It has been shown [19] that the spin-wave damping is strongly nonlinear, and it is active for vortex velocities larger than a certain threshold velocity, v_{th}. Below this velocity the vortex may move ballistically.

We pursue the approach discussed in detail in [19]. Following the standard analytical continuation procedure (see, e.g., [21]), we derive the equation of motion for the vortex coordinate. Considering then a constant vortex velocity, perpendicular to the applied current, we put $v = (v, 0)$, and $f = (0, f)$ for simplicity. The result is the following [19]:

$$2\pi f = v \int d^2 k \, \frac{k_y^2}{k^4} \int d\omega \, \dot{\mathcal{Q}}_{k,\omega}^R \, \delta(\omega + k_x v) \tag{42}$$

where $\mathcal{Q}_{k,\omega}^R$ is the retarded continuation of $\mathcal{Q}_{k,\omega}$, and $\dot{\mathcal{Q}}_{k,\omega}^R = -i\omega \mathcal{Q}_{k,\omega}^R$. By using the expression (38) for the connected correlation function, we obtain (including the smooth cut-off [17]; $k_c^2 = 2\pi$)

$$\frac{f}{E_J} = \frac{v}{4} \int d^2 k \, e^{-k/k_c} \frac{k_y^2}{k^2} \, \delta(\omega_k + k_x v) + \delta(\omega_k - k_x v) \ . \tag{43}$$

This relation determines the (nonlinear) dependence of the vortex velocity on the external current.

The vortex velocity as a function of the current for several values of α and in the absence of external charges is shown in figure 7 (for the correlation length we have again used the Padé approximation $P_1^1(s)$, from equation (30)). It is apparent that the spin-wave damping is active only for velocities larger than a certain threshold v_{th}; for $v < v_{th}$ a constant-velocity solution of (43) exists only for zero current. This indicates the possibility of ballistic motion.
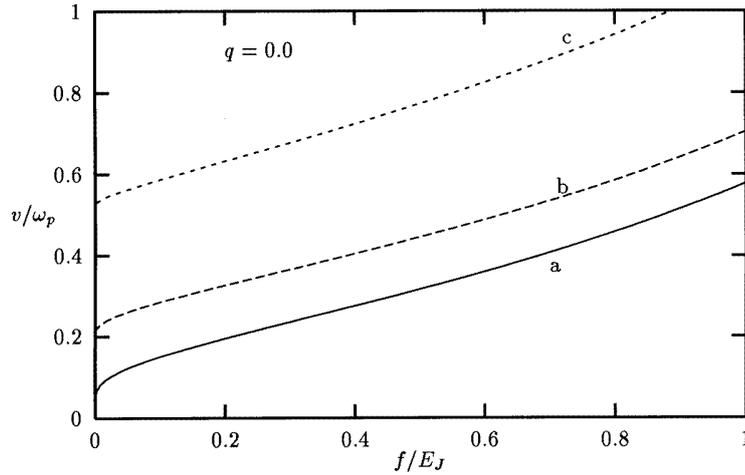
Figure 7. The vortex velocity v (in units of the plasma frequency) versus the driving current f/E_J in the absence of external charges and for different values of the parameter α (a: $\alpha = 0.0$; b: $\alpha = 0.9$; c: $\alpha = 1.1$).
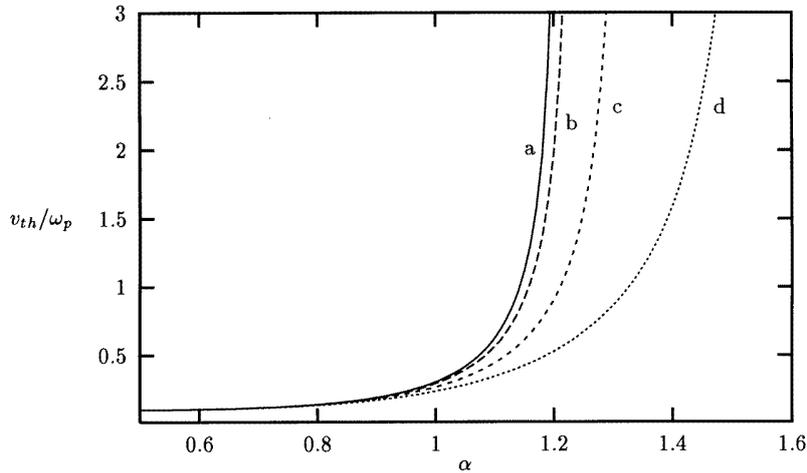

Figure 8. The threshold velocity v_{th} as function of α. The plots refer to different values of the offset charges. From a to d, q increases from 0.00 to 0.045 in steps of 0.015. All of the plots tend to the classical limit result, $v_{th}^{cl} \simeq 0.1\omega_p$, for $\alpha \to 0$.

For $\alpha \to 0$ (figure 7, curve a) the continuum model result [19] is obtained. In particular, the threshold velocity is given by $v_{th}^{cl} \simeq 0.1\omega_p$. On increasing the ratio E_J/E_C, a larger window for ballistic motion opens, as is obvious from figure 8 (curve a), where we show the threshold velocity versus α. At the transition, $\alpha = \alpha_c$, the vortex decouples completely from the spin waves, and v_{th} diverges.

The curves b–d in figure 8 show v_{th} versus α for different values of the offset charge. The threshold velocity for $\alpha \to 0$ approaches v_{th}^{cl} for all q, because the offset charges do

not affect the classical limit. When $\alpha \neq 0$, the threshold velocity depends strongly on the charge. In particular, v_{th} decreases with increasing q and, as a consequence, the critical value α_c moves to higher α.

The critical behaviour of v_{th} can be compared to that of the vortex mass M_v. For large E_J/E_C, the vortex mass and the threshold velocity approach a constant value, while close to the phase transition, M_v decreases and v_{th} increases rapidly. In particular, at the critical value α_c, the mass vanishes and the threshold velocity diverges, and with increasing q, M_v increases and v_{th} decreases. We conclude that offset charges frustrate the array, favouring superconductivity (increasing M_v), but reducing the ballistic window (decreasing v_{th}).

5.3. The linear response of a moving vortex

Given the above (or any other) approximation of the charge–charge correlation function, equation (39), it is straightforward to write down the nonlinear equation of motion for the vortex coordinate; the result (we ignore the Hall contribution, compare [8], chapter 8) is given in [19], equation (10), provided that we identify $g^R(\boldsymbol{k}, \omega)$, defined there, with $\mathcal{Q}^R(\boldsymbol{k}, \omega)/k^2$. Furthermore, we assume that in addition to the constant external current, which leads to a constant vortex velocity in the x-direction, there is a small oscillating current at frequency ω. Thus we put $\boldsymbol{r}(t) = (vt + \delta x, \delta y)$, linearize the equation of motion with respect to $\delta \boldsymbol{r}(t) = (\delta x, \delta y)$, and define a frequency- and velocity-dependent vortex mass tensor as a generalization of equation (36). This quantity is *not* directly related to the analytic continuation of equation (35), except for for $v \to 0$, where

$$M_v \to M_v^R = \frac{1}{2} \int \frac{\mathrm{d}^2 k}{k^2} \mathcal{Q}^R(\boldsymbol{k}, \omega). \tag{44}$$

The real part of this quantity (which is even in ω) increases quadratically for small ω, diverges logarithmically at $\omega = \omega_p$, becomes negative for $\omega \sim \omega_p (1 + 4\pi \xi^2)^{1/2}$, and decreases $\sim -M_{ES}/\omega^2$ for extremely large frequencies. The details depend on the form of the cut-off. Furthermore, its imaginary part (which is odd in ω) is finite (and $\sim M_{ES}/\xi^2$) only in the frequency range where real spin waves exist, i.e. between ω_p and $\sim \omega_p (1 + 4\pi \xi^2)^{1/2}$. Details will be presented elsewhere.

6. Summary

We have studied the superconductor–insulator transition in a Josephson junction array with a uniform static background of offset charges q, in the limit of a long-ranged Coulomb interaction, by an analytical method similar to a low-temperature expansion. We have shown that the transition strongly depends on the external charge. It moves quickly from the value $\alpha_c(q = 0) \simeq 1.2$ to higher α with increasing q, and seems to disappear when the magnitude of the offset charge is strong enough: a finite q frustrates the charge order in the array and strongly stabilizes superconductivity.

We also studied various aspects of the vortex dynamics. We have calculated the vortex mass, confirming the classical result, M_{ES}, independently of q, in the limit of a dominant Josephson coupling energy ($\alpha \to 0$). Close to the phase transition the vortex mass decreases and vanishes at a critical value α_c.

We eventually investigated the vortex motion driven by an external current. It was confirmed that nondissipative motion is only possible for velocities below a certain threshold v_{th}, while for $v > v_{th}$, the creation of spin-wave excitations leads to a constant velocity in the presence of a constant current. The threshold velocity becomes larger as α approaches

α_c, which means that ballistic motion of vortices is more likely to be observable in arrays that are close to the superconductor–insulator phase transition. Furthermore, offset charges strongly reduce the window for ballistic motion.

Acknowledgments

References

[1] For a general discussion of 2-D junction arrays, see, e.g.,
    Mooij J E and Schön G 1992 *Single Charge Tunnelling (NATO ASI series B, vol 294)* ed H Grabert and M H Devoret (New York: Plenum) p 275
[2] van der Zant H S J, Fritschy F C and Mooij J E 1992 *Europhys. Lett.* **19** 541
    van der Zant H S J, Fritschy F C, Ellion W E, Geerligs L J and Mooij J E 1992 *Phys. Rev. Lett.* **69** 2971
[3] Fazio R and Schön G 1991 *Phys. Rev.* B **43** 5307
[4] Kissner J G and Eckern U 1993 *Z. Phys.* B **91** 155
[5] Fazio R, van Otterlo A and Schön G 1994 *Europhys. Lett.* **25** 453
    van Otterlo A 1994 *PhD Thesis* University of Karlsruhe
    van Otterlo A, Fazio R and Schön G 1994 *Physica* B **203** 504
[6] Roddick E and Stroud D H 1993 *Phys. Rev.* B **48** 16 600
[7] van Otterlo A, Wagenblast K-H, Fazio R, and Schön G 1993 *Phys. Rev.* B **48** 3316
    Bruder C, Fazio R, Kampf A P, van Otterlo A and Schön G 1992 *Phys. Scr.* T **42** 159
    van Otterlo A and Wagenblast K-H 1994 *Phys. Rev. Lett.* **72** 3598
[8] Fazio R, van Otterlo A, Schön G, van der Zant H S J and Mooij J E 1992 *Helv. Phys. Acta* **65** 228
[9] Luciano G, Eckern U and Kissner J G 1996 *Europhys. Lett.* at press
[10] Villain J 1975 *J. Physique* **36** 581
[11] José J V, Kadanoff L P, Kirkpatrick S and Nelson D R 1977 *Phys. Rev.* B **16** 1217
[12] Domb C 1974 *Phase Transitions and Critical Phenomena* vol 3, ed C Domb and M S Green (London: Academic) p 225
[13] Chui S T and Weeks J D 1976 *Phys. Rev.* B **14** 4978
[14] van Beijeren H and Nolden I 1987 *Structure and Dynamics of Surfaces II* ed W Schommers and P von Blanckenhagen (Heidelberg: Springer) p 259
    Nienhuis B 1987 *Phase Transitions and Critical Phenomena* vol 11, ed C Domb and J L Lebowitz (London: Academic) p 1
[15] Guttmann A J 1987 *Phase Transitions and Critical Phenomena* vol 13, ed C Domb and J L Lebowitz (London: Academic) p 1
[16] Larkin A I, Ovchinnikov Yu N and Schmid A 1988 *Physica* B **152** 266
[17] Eckern U and Schmid A 1989 *Phys. Rev.* B **10** 6641
[18] van der Zant H S J, Fritschy F C, Orland T P, and Mooij J E 1992 *Europhys. Lett.* **18** 343
[19] Eckern U and Sonin E B 1993 *Phys. Rev.* B **47** 505
[20] Geigenmüller U, Whan C B and Lobb C J 1993 *Phys. Rev.* B **47** 348
[21] Eckern U, Schön G and Ambegaokar V 1984 *Phys. Rev.* B **30** 6419